Lattice energies and structural distortions in $Pb(Zr_xTi_{1-x})O_3$ solid solutions

2002 J. Phys.: Condens. Matter 14 8131

(http://iopscience.iop.org/0953-8984/14/34/331)

INSTITUTE OF PHYSICS PUBLISHING JOURNAL OF PHYSICS: CONDENSED MATTER

J. Phys.: Condens. Matter **14** (2002) 8131–8143 PII: S0953-8984(02)37357-0

Lattice energies and structural distortions in $Pb(Zr_xTi_{1-x})O_3$ solid solutions

G A Rossetti Jr[1,2,5], J P Cline[3], Y-M Chiang[2] and A Navrotsky[4]

[1] Research and Development Group, Continuum Photonics Incorporated, 45 Manning Road, Billerica, MA 01821, USA
[2] Department of Material Science and Engineering, Massachusetts Institute of Technology, Cambridge, MA 02139, USA
[3] Ceramics Division, National Institute of Standards and Technology, Gaithersburg, MD 20899, USA
[4] Thermochemistry Facility, Department of Chemical Engineering and Materials Science, University of California, Davis, CA 95616, USA

E-mail: gar@ContinuumPhotonics.com

Received 23 May 2002
Published 15 August 2002
Online at stacks.iop.org/JPhysCM/14/8131

Abstract

The changes in Madelung and non-electrostatic energies of $Pb(Zr_xTi_{1-x})O_3$ (PZT) solid solutions in the high-symmetry ($Pm3m$) phase have been calculated using the heats of formation from the oxides. The non-electrostatic contribution (ΔE_N) decreases with decreasing x and becomes negative for compositions $x \leqslant 0.35$, corresponding to perovskite tolerance factors $t \geqslant 1$. Correlation of the strong increase in tetragonal distortion in the ferroelectric phase with more exothermic values of ΔE_N suggests a softening of short-range repulsions for Ti-rich compositions. The influence of complex solid solution behaviour on the character of $Pm3m \leftrightarrow P4mm$ transition is investigated by high-temperature specific heat and unit-cell parameter measurements. The implications of the thermochemical results with respect to mean-field theoretical descriptions of lattice instabilities and phase boundaries in the PZT system are briefly discussed.

1. Introduction

Solid solutions of $Pb(Zr_xTi_{1-x})O_3$ (PZT) have been widely exploited in ceramic materials and devices because of their ferroelectric and piezoelectric properties. At high temperatures, the symmetry of the cubic prototype is $Pm3m$ for all values of zirconium incorporation, x. At room temperature and ambient pressure, the end-member $PbTiO_3$ is ferroelectric with tetragonal symmetry $P4mm$, while $PbZrO_3$ is antiferroelectric with orthorhombic symmetry $Pbam/Pba2$. For many years it has been accepted that the intermediate solid solution

[5] Author to whom any correspondence should be addressed.

compositions adopt orthorhombic, tetragonal, and rhombohedral ($R3m$ or $R3c$) symmetries according to the published composition–temperature (x–T) phase diagram of Jaffe *et al* [1]

However, since the discovery by Noheda *et al* [2] of compositions close to the morphotropic phase boundary (MPB) with monoclinic (Cm) symmetry, it has become apparent that the phase diagram in PZT is more complex than previously believed. Subsequent work has also revealed monoclinic phases in the related MPB systems $Pb(Mg_{1/3}Nb_{2/3})O_3$–$PbTiO_3$ and $Pb(Zn_{1/3}Nb_{2/3})O_3$–$PbTiO_3$, and there is very recent evidence that monoclinic phases with antiferrodistortive transitions also appear near the MPB in PZT [3, 4]. These findings are of great importance, as they indicate that all of the ferroelectric species predicted by the symmetry arguments of Shuvalov [5] may be accessible in these mixed systems under appropriate conditions. In addition to their considerable importance for technological applications such as piezoelectric transducers, phases of monoclinic, and potentially triclinic, symmetry pose challenges for theoretical approaches to the description of lattice instabilities in the PZT system.

Prior attempts to describe the relations among ferroic phases in the PZT system have utilized an extension of the mean-field approximation of the Landau theory, as first applied to the ferroelectric perovskite $BaTiO_3$ by Devonshire [6] with the series expansion in the order parameter (spontaneous polarization) truncated somewhat arbitrarily at terms of sixth order. This theory, generalized to account for the MPB and for the cell-doubling transformations in the rhombohedral and orthorhombic phase fields in PZT [7], does not predict the existence of the observed monoclinic phase. It has been shown recently that the monoclinic phase appears in the simple Devonshire theory only if the expansion in the order parameter is carried to terms of eighth order, and that triclinic phases only appear when twelfth-order terms are retained [8]. Implicit in these phenomenological theories is the assumption that the mixing characteristics of PZT solid solutions can be regarded as a minor perturbation that may modify the microscopic crystal interaction parameters but otherwise not affect the nature of physical processes controlling the structural transitions [9]. Alternatively, monoclinic phases arise naturally from first-principles effective Hamiltonian approaches in just the composition region found experimentally [10].

In studies of phase stability in PZT, there have been attempts to produce strictly homogeneous polycrystalline materials with respect to the distribution of Zr and Ti ions on octahedral positions of the perovskite structure [11, 12]. Although this can be accomplished at the limit of detectability of lattice parameter and x-ray profile broadening measurements made using conventional laboratory diffraction instruments, there is evidence to suggest that PZT solid solutions inherently exhibit more complex behaviour:

(1) lead oxide (PbO) activities over the cubic perovskite are not linear with composition (as expected for an ideal solution) at temperatures below 1330 K, particularly in the tetragonal phase field [13];
(2) the Curie temperature does not renormalize in the predicted way with cation displacement across the solid solution series, and there appears to be a 'plateau effect' on the $PbZrO_3$ side of the diagram for sufficiently small Ti substitutions [14]; and
(3) poled monophasic samples near the MPB show clear evidence of unmixing and eventual decomposition to coexisting tetragonal and rhombohedral phases at long (one year) aging times [15].

Very recently we have measured the heats of formation of PZT compositions across the nominally cubic solid solution series directly by high-temperature oxide melt solution calorimetry [16]. There exists a positive heat of mixing that can be described qualitatively by a regular solution model, but with an unexpectedly large value of the interaction parameter ($W \approx 40 \pm 4.7\,\mathrm{kJ\,mol^{-1}}$). If the regular solution model were strictly valid, this would predict a

symmetrical solvus at $W/2R = 2400$ K, where R is the gas constant. Since such a solvus with obvious unmixing is not seen on the timescale of normal laboratory experiments, we conclude that the simple regular solution model is not valid as a microscopic description. Instead complex solution behaviour at the level of individual polyhedra is inherent in the high-symmetry phase and attributable in part to differences in the d-state hybridization characteristics of Ti–O and Zr–O bonds. First-principles calculations of the electronic density of states in the local density approximation (LDA) show that the appearance of the ferroelectric instability in $PbTiO_3$ is intimately connected with the hybridization of the Ti d states [17]. Without contributions from covalent bonding effects, the Coulomb energy favours the ferroelectric distortion, but short-range repulsions remain strong enough to stabilize the cubic phase. Thus the simple regular solution model is inadequate even for the high-temperature, high-symmetry solid solution.

To further explore energetics in PZT, we have analysed previously measured heats of formation of PZT solid solutions in the cubic ($Pm3m$) phase using the lattice energy approach applicable to a large number of perovskite compounds [18]. Using this approach, we separate the long-range electrostatic (Coulomb) forces from non-electrostatic forces dominated by short-range repulsive interactions, but to which other terms also contribute. The results are related to the degree of distortion from the ideal perovskite structure of PZT compositions across the solid solutions series, as well as to the corresponding ferroelastic strain. New results of high-temperature x-ray diffraction measurements made near the $Pm3m \leftrightarrow P4mm$ transition temperature (T_t) are also reported and are correlated with the calorimetric data. Some implications of these observations concerning the complex nature of the PZT phase diagram, and the anomalous transition behaviour at the Curie temperature, previously attributed to mean-field tricritical points (TCPs), are discussed.

2. Experimental details

The complete details of specimen preparation, experimental protocols, and data reduction methods have been previously described [16, 19–21], so only a brief summary is given here. The PZT materials were obtained from chemically derived precursors crystallized in sealed Pt capsules at 1323 K. High-resolution x-ray diffraction and electron probe microanalysis were used to ensure phase purity, stoichiometry, and bulk chemical homogeneity in the samples. We note that the fluctuations in the distribution of Ti and Zr measured for these specimens (<0.2 at.% or 0.5 wt% as oxides) were quite small.

Heats of formation of PZT from the component oxides (PbO, ZrO_2, TiO_2) were measured at 973 K using a twin Calvet solution calorimeter and computed from thermochemical cycles with a propagated error of ± 2 kJ mol^{-1}. The specific heat (C_P) measurements were made using a differential scanning calorimeter with an absolute accuracy of $\pm 2\%$ in C_P and a temperature accuracy of $\pm 1^\circ$. Transition enthalpies and entropies were determined by appropriate integration of the specific heat data.

X-ray powder diffraction data were acquired on a Bragg–Brentano diffractometer using strictly monochromatic Cu $K\alpha_1$ radiation and a scanning linear position-sensitive detector (PSD) calibrated for line position and profile shape using a lanthanum hexaboride (LaB_6) reference standard. At a step increment of 0.01° 2θ, the corresponding count time of the PSD was 280 s/step. With this configuration, the instrumental resolution at $20^\circ \leqslant 2\theta \leqslant 100^\circ$ was <0.080° 2θ. For the high-temperature work, a tantalum hot stage operating under helium as a cover gas was used, and the measurements were made on cooling. At a common temperature $(T_t - T) = 12$ K relative to the $Pm3m \leftrightarrow P4mm$ transition, the breadth of the 200 reflections occurring at ≈45° 2θ for samples with $x = 0.00$–0.40 was $0.057^\circ \pm 0.015^\circ$ 2θ, comparable to the instrumental broadening of 0.067° 2θ measured at this angle at ambient temperature.

3. Data analysis

For an ionic crystal, the internal (lattice) energy was separated into two terms, $E = E_M + E_N$, where E_M is the electrostatic or Madelung energy and E_N contains all the other terms, of which the repulsive interaction is the largest positive term, but to which van der Waals, vibrational, and directional (covalent) bonding terms may also contribute. The van der Waals and vibrational (zero-point) energy terms typically contribute $<1\%$ each to E and, being of opposite sign, tend to cancel one another. We note that the contribution of the pressure–volume term to the enthalpy (ΔH) under the present conditions is negligible. Consequently, the internal energy differences on formation of PZT solid solutions from the component oxides, according to the reaction $AO + BO_2 = ABO_3$, can be approximated by $\Delta H_f(973\ \mathrm{K}) \cong \Delta E = \Delta E_M + \Delta E_N$ where ΔE_M is the difference in Madelung energy between products and reactants and ΔE_N is the difference in the non-electrostatic terms. If the term ΔE_M is calculated from known Madelung constants and interatomic distances of crystalline AO, BO_2, and mixed ABO_3, then ΔE_N may be determined from the experimental heats of formation [18].

The Madelung energies were computed from

$$E_M = [Z+, Z-]N_A A e^2/(4\pi\varepsilon_0 R_0) = 1390[Z+, Z-]A/R_0 \qquad (\mathrm{kJ\ mol^{-1}})$$

where A is the Madelung constant, Z the formal ionic charge, N_A is Avogadro's number, e is the electronic charge, and ε_0 is the permittivity of free space. R_0 is the shortest interatomic distance in the crystal expressed in ångstrom units. Here, E_M of AO was identified with that of PbO (litharge structure) and E_M of BO_2 with that of the composition-weighted average $x \cdot ZrO_2$ (baddeleyite structure) and $(1-x) \cdot TiO_2$ (rutile structure) for various values of x. The Madelung energy of the cubic perovskites PZT were calculated by taking $R_0 = a/2$, where a is the lattice parameter measured in the cubic phase at 823 K ($a = 3.96$ Å for $PbTiO_3$ and $a = 4.16$ Å for $PbZrO_3$) with a linear variation between the end-members according to Vegard's law as observed experimentally [11].

The distortions of PZT with respect to the ideal cubic perovskite are controlled by the tolerance factor $t = (r_A + r_O)/[(\sqrt{2})(r_B + r_O)]$ where r_A, r_B are the cation radii on the 12 coordinate and octahedral lattice sites of the cubic ABO_3 perovskite structure and r_O is the oxygen anion radius in sixfold coordination [22]. For the ideally close-packed cubic structure, $t = 1$. Alternatively, the apparent contraction of the octahedral sublattice with respect to the ideal perovskite can be quantified by $\Delta a = (a_{calc} - a_{meas})$ with $a_{calc} = 2(r_B + r_O)$. The ferroelastic distortions (spontaneous strains) were calculated in the various phases from the cell parameters as $(c/a) - 1$ for the tetragonal compositions and $(90 - \alpha)/90$ for the rhombohedral compositions [21, 23]. To facilitate comparison of the ferroelastic distortions with those of orthorhombic $PbZrO_3$, the spontaneous strain for the latter was calculated on the basis of a pseudo-tetragonal cell with $c/a < 1$ [24].

To determine unit-cell parameters for tetragonal compositions at temperatures near the $Pm3m \leftrightarrow P4mm$ transition point, the x-ray diffraction profiles were analysed with a two-peak model fitted with a split Pearson distribution function. The Pearson exponents were all close to unity, suggesting predominantly Lorentzian peak broadening, although given the apparent complexity of the solid solution system, no structural inference should be drawn from this observation. The two-peak model was used both below and above the transition point. The lowest temperature to which the cubic phase persisted could be easily identified by an abrupt change in the ratio of the integrated intensities of peaks, which was close to the expected value of $I_{200}/I_{002} = 2$ in the tetragonal phase. Profile breadths (FWHM) near the transition were subsequently determined by fitting the profiles with a one-peak model in the appropriate phase.

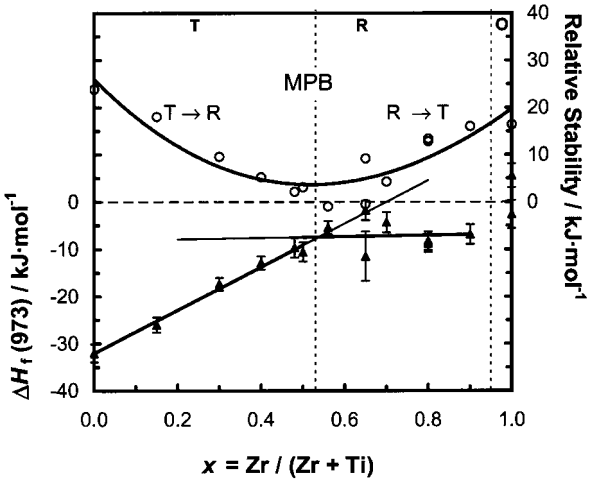

Figure 1. Heats of formation at 973 K of PZT solid solutions from the component oxides (solid triangles, left-hand scale). Predicted energy differences of the lower-temperature rhombohedral phase relative to the tetragonal phase in the tetragonal phase field and of the tetragonal phase relative to the rhombohedral phase in the rhombohedral phase field (open circles, right-hand scale).

4. Results and discussion

The heats of formation at 973 K of PZT solid solutions are plotted as a function of x in figure 1. Several trends are apparent. The delineation of the different trends observed in ΔH_f with respect to x correspond roughly with the phase boundaries of the x–T diagram, and so suggest that the heats of formation in the cubic phase at 973 K reflect energy differences related to the displacive transitions observed at lower (<765 K) temperatures. First, the x-dependence of ΔH_f decreases (becomes more exothermic) in the tetragonal phase field with decreasing values of x. In contrast, there is almost no variation with composition in the rhombohedral phase ($\Delta H_f \approx -7$ kJ mol^{-1}). The heat of formation for orthorhombic $PbZrO_3$ is zero within experimental error. Extrapolation of ΔH_f into opposing phase fields suggests that tetragonal $PbTiO_3$ is 24 kJ mol^{-1} more stable than a hypothetical $PbTiO_3$ modification with rhombohedral symmetry. Alternatively, rhombohedral $PbZrO_3$ is 16 kJ mol^{-1} more stable with respect to a hypothetical $PbZrO_3$ modification with tetragonal symmetry. The stabilities of tetragonal and rhombohedral phases relative to one another at intermediate compositions are also shown in figure 1, and differ by only several kilojoules per mol. The energy differences are small (<1 kJ mol^{-1}) near the MPB, suggesting that phases with lower symmetries must therefore lie very close in energy, beyond the resolution of our measurements.

Figure 2 shows the variation of the change in Madelung and non-electrostatic energies as a function of the tolerance factor t. It is seen from the figure that if t is qualitatively regarded as a measure of bond length mismatch in the cubic perovskite, the non-electrostatic energy becomes less favourable (more endothermic) with increasing absolute values $|t - 1|$ for $t \leqslant 1$, while the change in Madelung energy becomes more favourable. The compensating contributions of ΔE_M and ΔE_N to the heats of formation suggest that the repulsive energy contribution dominates, becoming progressively more positive with increasing deviation from the ideal structure on the $PbZrO_3$ side of the diagram. For the composition ($x \cong 0.35$) corresponding to the ideal perovskite with $t \cong 1$, ΔE_M and ΔE_N are equal in magnitude and negative in sign. For increasing values of $t > 1$, the signs of ΔE_M and ΔE_N reverse, suggesting a softening of

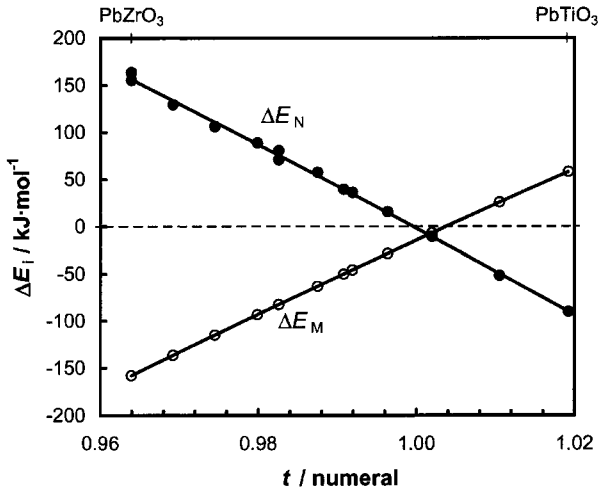

Figure 2. Change in the Madelung (ΔE_M) and non-electrostatic (ΔE_N) energies of PZT solid solutions versus perovskite tolerance factor in the cubic phase on formation from the component oxides.

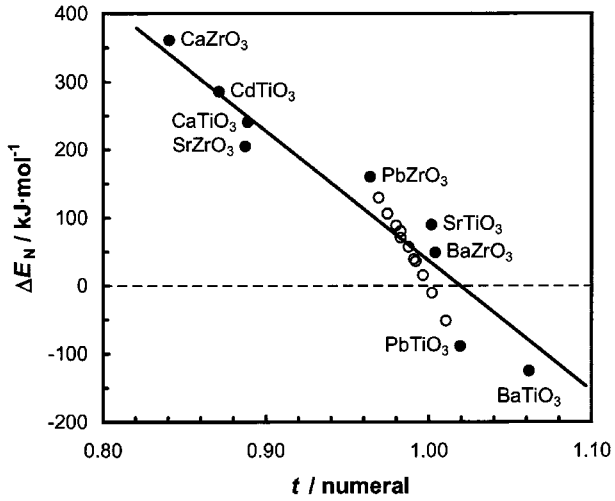

Figure 3. Change in non-electrostatic (ΔE_N) energies of PZT solid solutions versus perovskite tolerance factor as compared with other zirconate and titanate perovskite compounds. The ionic radii of the A-site cations used to calculate the tolerance factors are appropriately corrected for twelvefold coordination in the cubic perovskites and eightfold coordination in the orthorhombic perovskites. Ionic radii for the B-site cations and oxygen anions are for sixfold coordination.

the repulsive energy with respect to other contributions for the more $PbTiO_3$-rich compositions. It seems likely that this softening is related to a favourable covalent bonding component of ΔE_N, in agreement with expectations based on the LDA calculations for $PbTiO_3$ [17]. Indeed, as shown in figure 3, ΔE_N decreases more strongly with t in the PZT solid solution than expected on the basis of the trend observed for other zirconates and titanates (not containing lead) for which ΔE_N has been measured over a much broader range of t [18].

The relationship between ΔE_N and the ferroelastic distortion is shown in figure 4. Somewhat surprisingly, the spontaneous strain decreases with more endothermic (greater

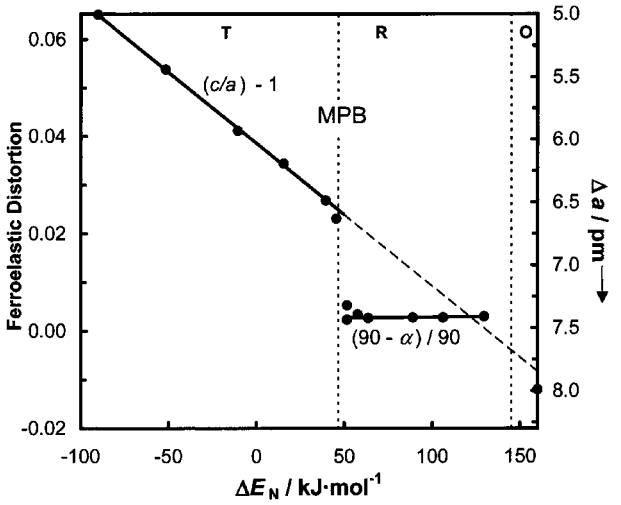

Figure 4. Dependences of the ferroelastic distortion (left-hand scale) and octahedral sublattice contraction Δa (right-hand scale) on the non-electrostatic (ΔE_N) energies of PZT solid solutions.

repulsive interaction) values of ΔE_N. The strong correlation between the two in the tetragonal phase field extrapolates to the $PbZrO_3$ side of the diagram for $x > 0.90$, where the heats of mixing are near zero. We also note that the spontaneous strain does not vary with the degree of deviation from the ideal perovskite as measured by the parameter Δa. The latter increases linearly with x, while the former shows an overall decrease with a discontinuity near the MPB as described above. From geometric (ionic size) arguments alone, we would expect the compositions with larger Δa to have larger ferroelastic distortions. However, our results show that any negative contribution of covalent bonding to ΔE_N is expected to decrease with increasing x, and so not favour large distortions, despite more exothermic values of the Coulomb contribution ΔE_M.

At intermediate compositions, $0.5 \leqslant x \leqslant 0.9$, there is no obvious correlation between ΔE_N and the spontaneous strain. It is important to note here that Rietveld refinement of powder neutron diffraction data on rhombohedral samples with $x = 0.60$–0.88 show better agreement with a model involving superimposed, random ⟨100⟩ Pb displacements than that achieved with a normal ⟨111⟩ long-range order model refined with anisotropic temperature factors [25]. It has also been found that if Ti and Zr cation shifts are treated independently, the difference between them is small at high values of x (low Ti concentration) but that the two diverge with decreasing x. For $x < 0.7$ the Ti shift increases rapidly while the Zr shift tends to zero. Moreover, the octahedral tilt and octahedral distortion behave in an anomalous way in the same range of composition [25]. This is consistent with our results showing that for these compositions, the heat of mixing is largest, indicating a tendency towards phase separation, and a possible change in the mode of accommodation of the delicately balanced repulsive and directional contributions to the non-electrostatic energy. In contrast, as discussed above, there is a smooth extrapolation of the spontaneous strain with ΔE_N from the tetragonal compositions to the compositions rich in Zr ($x > 0.9$).

To place the observed changes in lattice energy differences in context with the energetics of the structural phase transitions, we plot the enthalpies of the $Pm3m \leftrightarrow P4mm$ transition against the specific heat $C_P(x)$ measured in the high-symmetry phase for increasing values

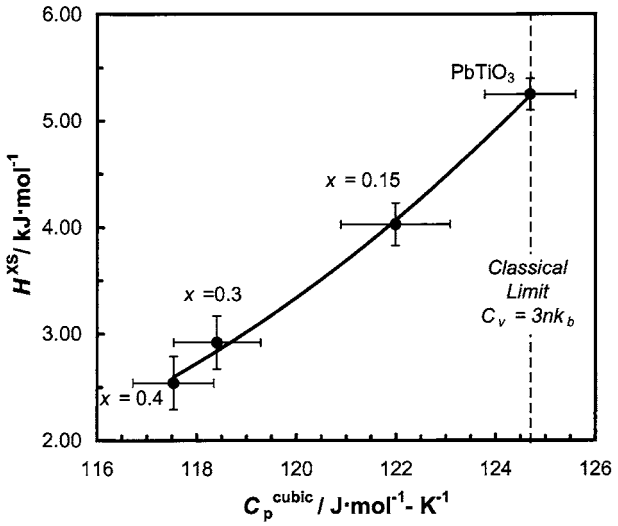

Figure 5. Excess enthalpies of the $Pm3m \leftrightarrow P4mm$ transition versus the specific heat $C_P(x)$ measured in the cubic phase for increasing values of x in PZT, near $t = 1$.

of x, in the vicinity of $t = 1$. The transition enthalpy is measured relative to the cubic phase by integration of the $C_P(T, x)$ curves corrected for the lattice background or 'hard-mode' specific heat. The 'excess' transition enthalpies so determined include contributions from the temperature dependence of the spontaneous polarization, as well as that from its discontinuity (latent heat) at the transition temperature.

As shown in figure 5, as C_P decreases from the Dulong–Petit limit (full equipartition excitation of vibrational modes) with increasing x, the transition enthalpy decreases. Because the changes in total transition enthalpy are on the order of 2–3 kJ mol^{-1}, the very closely balanced system energetics and cohesive properties (enthalpies, entropies, and volumes) will strongly influence the nature of the ferroelectric phase transition. This influence will be more pronounced near the MPB, given the relative phase stabilities predicted by the thermochemical data (figure 1). Because the vibrational density of states is related to the bonding configuration, we expect that non-idealities in the cubic solid solution to be reflected in the nature of the displacive transitions, which may renormalize in a complex way at various locations on the phase diagram.

In this connection, we note that there has been considerable controversy regarding whether the paraelectric–ferroelectric transition is continuous or discontinuous at various locations on the diagram, with significant disagreement regarding the general locations of any corresponding TCPs. In the mean-field theory, a change in the order of the transition is predicted to occur subject to the influence of an external parameter only if higher-order elastic terms, electrostrictive terms, or both are included in the Landau potential [26], or alternatively, if the lower-order terms adopt sufficiently renormalized values with respect to a variation in chemical composition in mixed crystals [27]. The applicability of the Landau theory to transitions near mean-field TCPs in solids both with and without impurities has been discussed in general terms by several authors [28, 29].

Figure 6(a) compares the ferroelastic distortion $(c/a) - 1$ versus $(T_t - T)$ for tetragonal compositions with various values of x. $PbTiO_3$ and samples with $x = 0.15$ and 0.30 have $t > 1$, while the sample $x = 0.40$ has $t < 1$. Figure 6(a) shows that the first-order character of

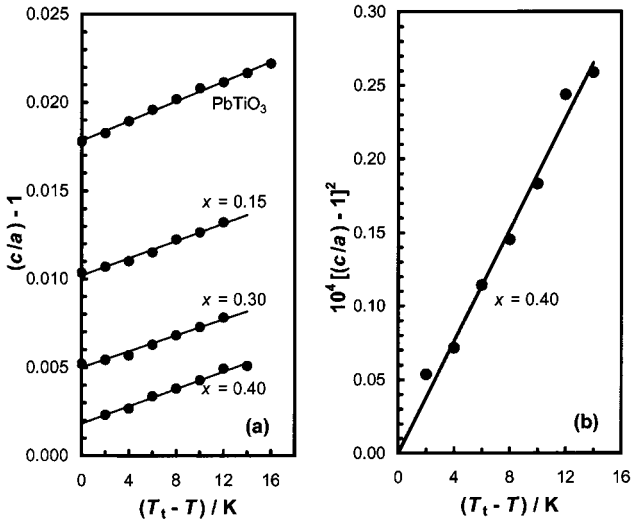

Figure 6. The ferroelastic distortion $(c/a) - 1$ versus $(T_t - T)$ for tetragonal compositions with various values of x (a); and the variation of the parameter $[(c/a) - 1]^2$ with $(T_t - T)$ for the sample with $x = 0.40$ (b).

the transition reduces strongly with increasing x (decreasing t), as judged by the discontinuity $\Delta(c/a) - 1$ at $(T_t - T) = 0$. The raw diffraction data for the samples with $x = 0.30$ and 0.40 are compared in figure 7. It is clear from inspection of the diffraction profiles that the transition for the sample with $x = 0.30$ ($t > 1$) is discontinuous, but that the same conclusion cannot be drawn for the sample with $x = 0.40$ ($t < 1$).

At a mean-field TCP the order parameter (spontaneous polarization, P) varies as $P \propto (T_t - T)^{1/4}$. Since the ferroelastic distortion is given by $(c/a) - 1 = qP^2$, where q is a (weakly temperature-dependent) electrostrictive constant, we expect $[(c/a) - 1]^2 \propto (T_t - T)$. That this relation is qualitatively obeyed for the sample with $x = 0.40$ is shown in figure 6(b). However, at the resolution of our measurements, it is difficult to ascertain whether the behaviour observed in figure 6(b) in fact results from proximity to a mean-field TCP, or rather, relates to a first-order phase change dominated by fluctuations due to complex mixing behaviour in the cubic phase.

Nonetheless, as shown in figure 8, the macroscopic behaviour of the excess entropy varies as expected in the Landau–Devonshire approximation, $\delta G^{xs}/\delta T = -S^{xs} \propto P^2$, or

$$-S^{xs} = (V_M)[2\varepsilon_0 C_{CW} q]^{-1}\{(c/a) - 1\}$$

where C_{CW} is the Curie–Weiss constant. The plot in figure 8 gives a slope of 112.5 J mol^{-1} K^{-1}, and substituting the value $q = 0.116$ m^4 C^{-2} [20] and the measured molar volume $V_M = 3.98 \times 10^{-5}$ m^3 mol^{-1} at T_t, we find $C_{CW} = 1.72 \times 10^5$ K. From these data, and noting that the measured hysteresis in transition temperature is less than 0.6 K [21] we may also calculate the quartic term of the Landau potential to be $\beta = -2.52 \times 10^7$ m^5 F^{-1} C^{-2}. These are to be compared to the values $C_{CW} = 1.25 \times 10^5$ K and $\beta = -7.79 \times 10^7$ m^5 F^{-1} C^{-2} determined by the same methods for $PbTiO_3$ [20]. However, even the phase change in pure lead titanate does not behave as expected for a purely displacive ferroelectric. In fact, x-ray adsorption fine-structure (XAFS) measurements suggest that the atomic displacements have at least two correlation length scales, one associated with local distortions and one associated with the order parameter [30].

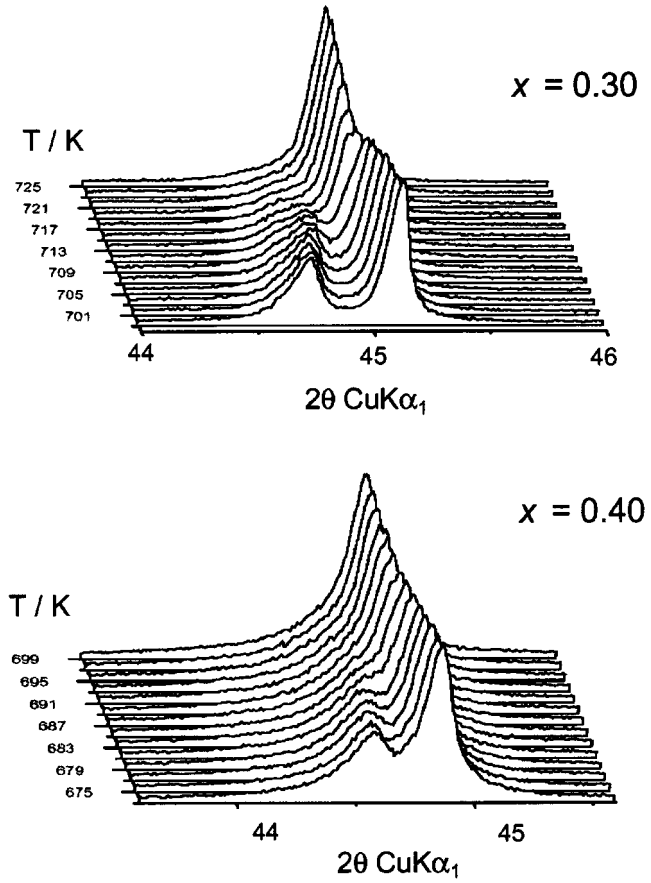

Figure 7. The 002/200 (tetragonal) and 200 (cubic) diffraction profiles for the samples with $x = 0.30$ (upper panel) and $x = 0.40$ (lower panel) as a function of temperature.

Accordingly, the inherently complex solid solution behaviour in the cubic phase of PZT might explain the observed anomalies in transition behaviour, first attributed to critical fluctuations [31], and later to the existence of mean-field TCPs at different values of x [21, 27, 32, 33]. Some additional evidence for this is given in figure 9, showing the x-ray profile breadths as a function of temperature for the sample with $x = 0.40$. As seen in the figure, there is an abrupt change in the temperature dependence of the profile breadths at T_t. It is seen that the cubic 200 reflection *increases* in breadth with decreasing temperature on approaching T_t, while the breadths of the tetragonal 200 and 002 profiles decrease as expected below T_t. Also, the tetragonal 002 reflections are significantly broader than the 200 reflections. It is known that the lattice parameter c is independent of x in the tetragonal phase field but that the lattice parameter a increases monotonically. Hence, these findings are not consistent with a fluctuation in composition Δx. Rather they support the existence of a non-uniform displacement of the octahedral cations Zr and Ti that continues at least 10 K into the nominally cubic phase.

Consequently, the physical significance of the negative sign of the quartic term as determined here for $x = 0.40$ is uncertain, especially given the temperature variation of the parameter $[(c/a) - 1]^2$ as shown in figure 6(b). Given the much higher resolution of our line profile measurements relative to those reported previously [12], the assertion [34] that the cubic-to-

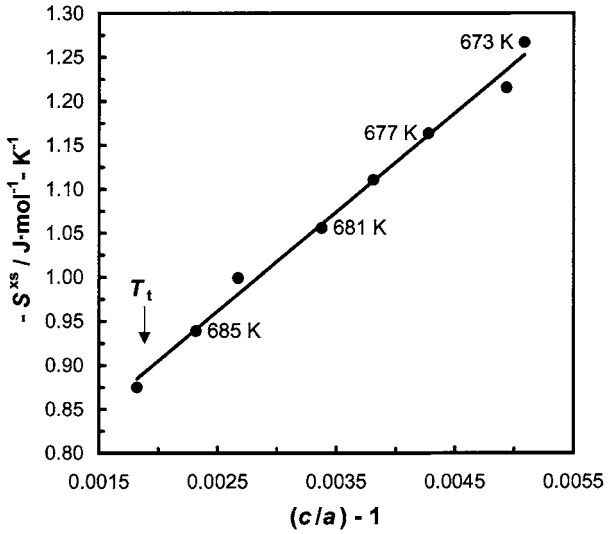

Figure 8. Excess entropy of the $Pm3m \leftrightarrow P4mm$ transition versus ferroelastic distortion $(c/a)-1$ for the sample with $x = 0.40$.

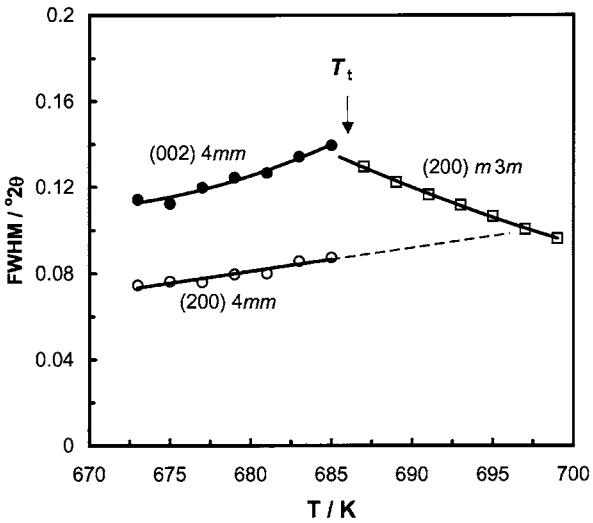

Figure 9. X-ray profile breadths (FWHM) for the sample with $x = 0.40$ as a function of temperature. Cubic 200 reflections (open squares), tetragonal 002 reflections (solid circles), tetragonal 200 reflections (open circles).

tetragonal transition is everywhere discontinuous, in the classical sense, remains in our opinion open to question. Rather, the observed behaviour is qualitatively more similar to that observed $BaTiO_3$ [35, 36] and $PbTiO_3$ [37] modified with foreign (isovalent and aliovalent) ions.

The above observations suggest that the perturbation caused by complex solution behaviour in PZT cannot be considered negligible with respect to the accessible ferroic symmetries on any arbitrary vertical line of the x–T diagram. Clearly, all solid solutions must exhibit some degree of positional disorder, complicating the lattice dynamical picture of

a single condensing soft mode in the harmonic approximation. Indeed, powder Raman spectra show vanishing values of the lowest E(1TO) mode for tetragonal PZT compositions with $x \geqslant 0.25$, and there is an abrupt change in the appearance of the spectra in the rhombohedral phase field, where all bands become unusually broad [38].

Clearly, large high-quality crystals suitable for crystal structure determination and for inelastic neutron scattering, which have so far been unavailable, are needed to more fully resolve this question. Nevertheless, our results suggest that thermodynamic descriptions in which the chemical potential is not explicitly included as a variable of state (i.e. incompletely integrated thermodynamic potentials) may not have strict physical validity in describing the complex sequence of phase transitions recently observed in PZT and related systems. In this respect, first-principles approaches should prove more illuminating [39]. Alternatively, the present results suggest that phenomenological theories involving more complex order parameter schemes [40], with appropriate temperature and composition dependences, should retain practical utility for the macroscopic description of the observed phenomena, and for the related elasto-dielectric properties of interest for technological applications.

5. Conclusions

The changes in lattice energies on formation of cubic PZT solid solutions from the oxides show that the largely repulsive, non-electrostatic energy softens with decreasing value of x. It is proposed that this softening is connected with a favourable (exothermic) contribution of covalent bonding energy terms. The correlation of the non-electrostatic energy with the perovskite tolerance factor and ferroelastic strain suggests a close relationship of bonding effects with the diversity of structural distortions observed in PZT. It also appears that the cubic phase at 973 K contains vestiges, in both the structural and thermodynamic sense, of the different displacements of Ti and Zr inferred for the lower-symmetry phases at lower temperatures.

We also have shown directly that ferroic phases, especially near the MPB, are positioned very closely in energy ($\leqslant 1$ kJ mol^{-1}). Because of the delicately balanced energetics and complex solution behaviour in the cubic phase, even properly formulated Landau functions, though providing an adequate description of macroscopic behaviour, may suffer deficiencies with respect to the physical significance of the expansion terms. First-principles calculations are needed to relate microscopic or semi-microscopic parameters to the observed Landau coefficients. Thermochemical studies of other MPB systems, such as $Pb(Mg_{1/3}Nb_{2/3})O_3$–$PbTiO_3$ and $Pb(Zn_{1/3}Nb_{2/3})O_3$–$PbTiO_3$, should also be helpful in more fully understanding the phase diagrams and the relation of structure and bonding in these complex, but technologically important, materials.

Acknowledgments

Partial support of this work by the Defense Advanced Research Projects Agency under contracts administered by the US Air Force Office of Scientific Research (grant No F49620-99-2-0332) is gratefully acknowledged. The calorimetric studies benefited from the infrastructure provided by CHiPR, the Center for High Pressure Research, an NSF Science and Technology Center.

References

[1] Jaffe B, Cook W R and Jaffe H 1971 *Piezoelectric Ceramics* (London: Academic) ch 7
[2] Noheda B, Cox D E, Shirane G, Gonzalo J A, Cross L E and Park S E 1999 *Appl. Phys. Lett.* **74** 2059

[3] Kiat J-M, Uesu Y, Dkhil B, Matsuda M, Malibert C and Calvarin G 1999 *Phys. Rev.* B **65** 064106
[4] Ranjan R, Mishra R S K and Pandey D 2002 *Phys. Rev.* B **65** 060102(R)
[5] Shuvalov L A 1970 *J. Phys. Soc. Japan* **28** 38
[6] Devonshire A F 1949 *Phil. Mag.* **40** 1040
[7] Haun M J, Furman E, Jang S J and Cross L E 1989 *Ferroelectrics* **99** 13
[8] Vanderbilt D and Cohen M H 2001 *Phys. Rev.* B **63** 094108
[9] Yurkevich V E and Rolov B N 1972 *Phys. Status Solidi* b **52** 335
[10] Zhong W, Vanderbilt D and Rabe K M 1995 *Phys. Rev.* B **52** 6301
Bellaiche L, Garcia A and Vanderbilt D 2000 *Phys. Rev. Lett.* **84** 5427
[11] Kakegawa K, Mohri J, Takahashi T, Yamamura H and Shirasaki S 1977 *Solid State Commun.* **24** 769
[12] Singh A P, Mishra S K, Pandey D, Prasad C H D and Lal R 1993 *J. Mater. Sci.* **28** 5050
[13] Härdtl K H and Rau H 1969 *Solid State Commun.* **7** 41
[14] Amin A, Newnham R E and Cross L E 1980 *Mater. Res. Bull.* **15** 721
[15] Kakegawa K, Mohri J, Shirasaki S and Takahashi K 1982 *J. Am. Ceram. Soc.* **10** 515
[16] Rane M V, Navrotsky A and Rossetti G A Jr 2001 *J. Solid State Chem.* **161** 402
[17] Cohen R E 1992 *Nature* **358** 136
[18] Takayama-Muromachi E and Navrotsky A 1988 *J. Solid State Chem.* **72** 244
[19] Rossetti G A Jr, Cross L E and Cline J P 1995 *J. Mater. Sci.* **30** 24
[20] Rossetti G A Jr, Cline J P and Navrotsky A 1998 *J. Mater. Res.* **13** 3197
[21] Rossetti G A Jr and Navrotsky A 1999 *J. Solid State Chem.* **144** 188
[22] Shannon R D 1976 *Acta Crystallogr.* A **32** 751
[23] Jaffe B, Roth R S and Marzullo S 1955 *J. Res. NBS* **55** 239
[24] Sawaguchi E 1953 *J. Phys. Soc. Japan* **8** 615
[25] Corker D L, Glazer A M, Whatmore R W, Stallard A and Fauth F 1998 *J. Phys.: Condens. Matter* **10** 6251
[26] Benguigui L 1973 *Phys. Status Solidi* b **60** 835
[27] Whatmore R W, Clarke R and Glazer A M 1978 *J. Phys. C: Solid State Phys.* **11** 3089
[28] Aleksandrov K S and Flerov I N 1979 *Sov. Phys.–Solid State* **21** 195
[29] Levanyuk A P, Minyukov S A and Vallade M 1993 *J. Phys.: Condens. Matter* **5** 4419
[30] Sicron N, Ravel B, Yacoby Y, Stern E A, Dogan F and Rehr J J 1994 *Phys. Rev.* B **50** 13 168
[31] Clarke R and Glazer A M 1974 *J. Phys. C: Solid State Phys.* **7** 2147
[32] Haun M J, Furman E, McKinstry H A and Cross L E 1989 *Ferroelectrics* **99** 27
[33] Eremkin V V, Smotrakov V G and Fesenko E G 1990 *Ferroelectrics* **110** 137
[34] Mishra S K, Singh A P and Pandey D 1997 *Phil. Mag.* B **76** 2130
[35] Darlington C N W and Cernik R J 1991 *J. Phys.: Condens. Matter* **3** 4555
[36] Darlington C N W and Cernik R J 1992 *J. Phys.: Condens. Matter* **4** 4387
[37] Rossetti G A Jr, Rodriguez M A, Navrotsky A, Cross L E and Newnham R E 1995 *J. Appl. Phys.* **77** 1683
[38] Burns G and Scott B A 1970 *Phys. Rev. Lett.* **25** 1191
[39] Strukov B A and Levanyuk A P 1998 *Ferroelectric Phenomena in Crystals: Physical Foundations* (Berlin: Springer) ch 7
[40] Salje E K H 1991 *Acta Crystallogr.* A **47** 453